ORIGINAL

Combined impact of moisture and temperature on cellulose nanocrystal interface degradation by molecular dynamics simulation

Jialiang Li[1] · Yujun Li[1] · Zhengdao Li[1] · Yongkang Wang[1] · Jianjun Jiang[1]

Abstract

Cellulose nanocrystals (CNCs), derived from abundant natural cellulose, possess exceptional properties including low weight, bioavailability, and high mechanical performance. During shear loading, CNCs exhibit unique stick–slip behavior, making them excellent toughening materials for CNC neat films and nanocomposite. However, the failure behavior at the interface under specific conditions, particularly moisture and temperature, remains unclear. The study utilized molecular dynamics (MD) simulations to quantitatively investigate the hydrothermal effect on the degradation of CNC interface. The degradation mechanism induced by moisture and temperature was indicated through the reduction of adhesive energy and peak force with the consideration of hydrogen bonds. The simulation results showed that the role of water molecules in the interfacial failure depends their content. Water acted as a binder at low moisture levels, while at high moisture levels, it acted as a lubricant. Besides, temperature had a more pronounced impact on the interfacial shear performance. Our simulation results can be used as input in micromechanical models to bridge the gap between the macroscopic and microscopic behavior of films and nanocomposites.

Introduction

Cellulose is one of the most abundant biological materials in the biosphere (Zhou et al. 2010). It is widely found in plant cell, tunicates, bacteria and algae (Bangar and Whiteside 2021; Jakob et al. 2022; Moon et al. 2011). Cellulose nanocrystal (CNC), a nanomaterial prepared by acid hydrolysis of cellulose feedstock, possesses many

✉ Yujun Li
  li.yujun@nwpu.edu.cn

✉ Jianjun Jiang
  jianjun@nwpu.edu.cn

[1] School of Mechanical Engineering, Northwestern Polytechnical Univercity, Xi'an 710072, People's Republic of China

Ⓐ Springer

qualities, including excellent mechanical properties, lightweight, biocompatibility, surface modifiability, optical properties and thermal properties (Bangar et al. 2022; Eichers et al. 2022; Zhao et al. 2022). Owing to these advantages, CNCs and their derivatives have been found as key ingredients of plenty applications in the fields such as tissue engineering (Patel et al. 2020), pharmaceutical synthesis (Yang and Li 2018), motion sensor (Huang et al. 2022), food packaging (Azeredo et al. 2017), 3D printing (Wang et al. 2018), optical films (Ren et al. 2022) and reinforcement in nanocomposite (Tang et al. 2017). CNCs exhibit good compatibility with various polymers, including cyclic olefin copolymer (COC), polyethylene glycol (PEG) and polylactic acid (PLA) (Kang et al. 2024; Shen et al. 2022; Xu et al. 2024). Their high aspect ratio facilitates efficient stress transfer from the polymer matrix to the CNCs, strengthening the composite material. In addition, CNCs can slip under shear stress and the overall damage degree of the nanocomposite could trail off as a result of stick–slip phenomenon (Ahmad et al. 2022; Molnár et al. 2018). Therefore, considerable attention should be paid to estimating the interfacial properties of CNCs.

In the practical application of materials, challenges related to moisture and temperature are inevitable. This conclusion holds particularly true for materials where interfacial properties significantly depend on moisture and temperature and impact overall performance (Li et al. 2019, 2022). Previous researches indicates that, in humid conditions, water molecules tend to accumulate at the interfaces, leading to an alteration in surface bonding (Zhou et al. 2015). Consequently, the mechanical properties of the interface, such as strength and fracture toughness, will degrade under the combined effects of moisture and temperature, which will further influence the total mechanical properties (Khoshkava and Kamal 2014; Naito and Nagai 2022). While moisture has limited direct impact on the internal structure of cellulose crystals, its presence within the material system can influence the overall integrity of the microstructure and, consequently, the fracture mechanisms (Jiang et al. 2019; Zhou et al. 2015).

CNCs are different from other nanoparticles where the 110 surfaces of CNCs are deeply hydrophilic, and as a result, it is easier for the CNC system to adsorb water (Adak and Mukhopadhyay 2018; Sinko and Keten 2015). Consequently, the moisture and temperature have a significant impact on the materials consisting of CNCs. Previous studies have shown that numerous hydrogen bonds form at the CNC interface. These bonds exhibit a dynamic destruction-restoration behavior during CNC shearing, contributing to the observed stick–slip phenomenon (Sinko and Keten 2014, 2015). The stick–slip phenomenon is a periodic motion observed when two contacting surfaces, like CNCs in this study, alternate between sticking together and then rapidly slipping past each other during shear. This cycle arises from the buildup and release of shear forces at the interface. It can strengthen the toughness of the interface (Meng and Shi 2021; Shishehbor et al. 2018; Zhu et al. 2015). The introduction of water molecules also involves the formation of hydrogen bonds between the CNC interface and alters the macroscale shear property. Thus, it becomes important to investigate the interfacial properties of CNCs and their mechanical responses under varying moisture and temperature conditions.

Characterizing interfacial properties at the nanoscale presents a significant challenge. Due to the inherent limitations of nanoscale measurements, these techniques

often capture the combined mechanical response of a material under multiple deformation modes, such as tension and shear. This inherent coupling makes it difficult to isolate and directly measure the intrinsic interfacial properties, such as strength under purely tensile or shear loading conditions. With the development of computational technology, molecular dynamics (MD) simulation has filled this gap. Sinko and Keten (2014, 2015) investigated the shear and tensile failure behavior of CNC interface through MD simulation. It was found that the 110–110 CNCs interface has a higher hydrogen bond density than 200–200 interface. Thus, the 110–110 interface possesses higher interfacial shear and tensile strength. Notably, during the shearing process of 200–200 interfaces, other intermolecular interactions like van der Waals provided more effects than hydrogen bonds. Furthermore, the tensile strength and shear strength of the interface decrease after inserting a layer of water molecules between the interface. Zhang et al. (2021b) systematically studied the stick–slip behavior of CNC interfaces dominated by hydrogen bonds. During shearing deformation, the interfacial stress, shear velocity, and the energy barrier were strongly associated with hydrogen bond density. It was also found that moisture lowers the interfacial friction and impacts the stick–slip behavior pattern of CNC interfaces. Due to the high hydrogen bond density between CNC surfaces, water molecules were more likely to affect their interfacial properties. Wei et al. (2018) studied the interfacial properties of 200–200 interfaces in wet environments modified by different methods. Through MD simulations, CNC modified with Na^+ had better moisture absorption performance, while the hydrophilicity degree of the interface shifted more significantly compared to $Meph_3P^+$ modification, and its interfacial shear strength and tensile strength increased due to the introduction of water molecules. Zhang et al. (2021a) used molecular dynamics simulation to comprehensively study the effects of moisture on the structure and mechanical properties of the wood cell wall which were composed of crystalline cellulose fibers and matrix. They found that the hydration could induce the degradation of the wood cell wall which was caused by the decrease in the mechanical properties of the matrix and fiber-matrix interface. He et al. (2023) employed molecular dynamics simulation to estimate the hygromechanics on the CNCs interface. Through numerical and theoretical methods, it was found that the moisture could change the local deformation mode and improve the load transferability at the interface. Another interesting phenomenon observed between the 200–200 interface was the capillary bridge built by water molecules which was also found by several investigators (Choi et al. 2021; Pan et al. 2019). Other studies on pure cellulose materials have shown that moisture increases the diffusion coefficient of water in microcrystalline cellulose and weakens the interaction between CNC interfaces (Garg et al. 2020; Sahputra et al. 2019). Moreover, in the reports of nanocomposites containing cellulose nanocrystals, moisture can weaken the interaction between cellulose and the substrate such as resin (Zhou et al. 2015). In general, although many studies have focused on the interface of CNCs, the knowledge gap still exists. There remains a need for a comprehensive study that can evaluate the separate and combined effects of moisture and temperature on the interfacial properties between CNCs. In practical applications, the impact of diverse environmental conditions, such as moisture and temperature, on the interfacial performance ought to be considered.

The objective of this study was to build MD models of CNC systems with water molecules and analyze the interfacial mechanical properties. Both interface peak force and adhesive energy were evaluated under varying moisture and temperature conditions. Specifically, the impacts of different moisture and temperature levels on the degrading effects of the CNCs interface were investigated from the perspective of interfacial interaction and mechanical properties. The combined effect of moisture and temperature was also discussed.

Materials and methods

Interface model construction

To estimate the effects of moisture and temperature on the interfacial mechanical properties of cellulose nanocrystals, MD simulations were conducted on CNC-CNC and CNC-water-CNC interfaces subjected to normal and shear loadings. The CNCs used in the present research had Cellulose Iβ crystal structure, the most stable CNC morphology, as shown in Fig. 1a. The crystal model was generated with the package Cellulose-builder (Gomes and Skaf 2012). Previous studies of CNCs have used both hexagonal (Fig. 1a) (Bregado et al. 2021; Oehme et al. 2015) and rectangular (Fig. 1b) (Wei et al. 2018) model systems. This work utilizes a rectangular model to establish the interfacial region of CNCs as depicted in Fig. 1c, d. The surfaces which form the interfacial region are labeled as Surface 1 (S1) and Surface 2 (S2). It should be noted that, the model employed in this study is a simplified representation of the complex interfacial configuration of CNCs rather than an exact replica. CNC with a size of 81.9×55×17.8 Å was selected to model the interface. The 200–200 interface was chosen as the model system for this study due to its reportedly higher
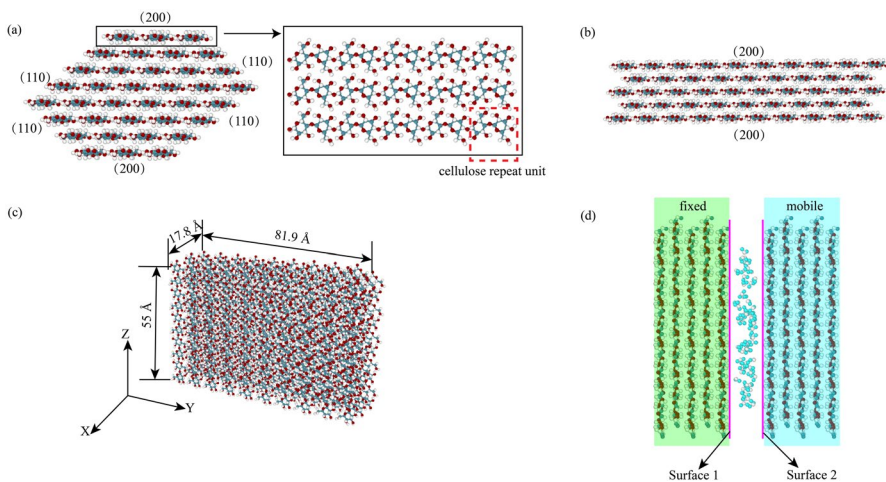

Fig. 1 Atomic structure of the MD model: **a** hexagonal model, **b** rectangular model, **c** the single model in this work, **d** the initial geometry configuration

sensitivity to moisture compared to the 110–110 interface (Sinko and Keten 2014). This characteristic makes it more interesting for studying the hydrothermal effects. It is convenient to form a water layer and trap more water molecules between the interfaces (Wei et al. 2018; Zhu et al. 2015). Each CNC comprised 48 chains with the dimensions shown in Fig. 1a. Two CNCs, including 20,448 atoms, were set parallel to create an interfacial region. The water molecules layer was randomly inserted into the initial configuration for subsequent simulation. In order to minimize the geometry's influence, ten independent interface models were used for each moisture and temperature condition. The TIP3P water model was employed in all simulations (Mianehrow et al. 2022).

The COMPASS force field was adopted in all the simulations. COMPASS is based on ab initio and has been widely used in previous cellulose MD studies (Du et al. 2021; Li et al. 2022; Long et al. 2022). The force field of the simulation models was assigned by Material Studio 8.0. The force field employed in this work encompasses both bonded and non-bonded interactions. Bonded interactions include covalent bonds, angles, and torsions. Non-bonded interactions are described by van der Walls (vdW) and Coulomb terms. Importantly, hydrogen bonds (h-bonds) are implicitly represented by incorporating their effects into the vdW and Coulomb interaction terms (Dri et al. 2015). The Lennard–Jones potential with 1.0 nm cutoff distance accounts for vdW interactions. Long-range Coulomb interactions are efficiently handled using the particle-mesh Ewald summation method, with an accuracy of 10^{-4}. The parameters for h-bonds in this work are defined based on a previous study, adopting a cutoff distance of 3.5 Å and a cutoff angle of 30° (Zhang et al. 2021a, b). The cutoff distance refers to the maximum allowable separation between the donor oxygen atom and the acceptor oxygen atom. The cutoff angle defines the maximum allowed deviation from the ideal angle formed by the accepter oxygen atom, donor oxygen atom and donor hydrogen atom. The simulations employ the canonical ensemble (NVT) a with constant number of atoms, volume, and temperature. The Nosé-Hoover thermostat maintains the temperature, and a timestep of 1 fs is used throughout. Periodic boundary conditions are applied in all directions. Finally, the simulation box dimensions are approximately 8.5 nm×8.5 nm×15 nm, with an additional blank space of 10 nm parallel to the interface and 4 nm normal to the interface. This ensures sufficient space to capture the entire shear and tensile fracture process, from initial failure to complete debonding. (Zhang et al. 2021a, b). The simulation was visualized by Ovito (Stukowski 2010) and the hydrogen bonds were estimated by VMD (Humphrey et al. 1996). All simulations are executed by LAMMPS (Thompson et al. 2022).

Equilibration and interfacial fracture simulations

Before all the simulations, the systems were first minimized through conjugate gradient algorithm. Prior to fracture simulation, the whole system was equilibrated for 2 ns. At the end of the equilibration, the temperature fluctuation is within the range of roughly 10 K and the energy fluctuation is within roughly 5000 kcal/mol·Å, indicating that the system has been stabilized. During the equilibration stage, the carbon atoms in the left

CNC were fixed in position, while the carbon atoms in the right CNC were set as a rigid body. This approach prevents unwanted torsion and rotation between the CNCs that could influence subsequent simulations. Additionally, our aim in this work is to capture the pure tensile and pure shear behavior (mode I and mode II) at the CNC interface. As a result, it is important to create a well-defined interface for the subsequent studies on interfacial performance, representing an ideal scenario. To create a moisture condition at the interface, a water layer with a width of 0.5 nm was introduced between the CNCs, as shown in Fig. 1b. The water layers were generated with random packing by *Packmol* (Martinez et al. 2009), and the moisture content at the interface was quantified using the moisture to dry mass ratio, which was determined through the following equation:

$$\text{moisture to dry mass ratio (\%)} = \frac{M_{\text{w}}}{M_{\text{C}}} \times 100\% \tag{1}$$

where M_{w} is weight of the water molecules between the CNCs, M_{C} is the original weight of the dry CNCs.

In the preliminary experiments, the water molecules remained absorbed on other surfaces during equilibration, which was also observed in a previous study (Garg et al. 2020).To maintain the water molecules between the interfacial region of CNCs, virtual walls were set around the CNCs to restrict the space for water molecules that could keep all the water molecules absorbed on the CNCs interfaces. The virtual walls used in this study were set for the purpose of maintaining the water molecules and creating a controlled moisture environment for our following investigation of interfacial properties.

In order to characterize the traction–separation behavior of CNC interface failure, the fracture simulation of CNC interface was utilized in two directions: normal to the interface which refers to tensile failure and parallel to the interface which refers to the shear failure. After equilibration of the CNC models, the carbon atoms in left CNC were fixed in the fracture simulation, whereas those in the right CNC were given a velocity boundary condition. The remainder of the system was completely free. Deformation velocities were 0.00001 Å /fs for both normal and parallel loading cases. In the fracture simulations, the load direction in tensile deformation is perpendicular to the CNCs interface and the load direction of shear deformation is parallel to the interface. The precise load direction allows for an accurate evaluation of the interfacial properties and investigation of the interfacial behavior. The timestep for all fracture simulations was set to 0.5 fs. Every 100 steps, the force and interactions between the CNCs were recorded for data collection. "Compute group/group" in LAMMPS was employed to calculate the adhesive energy and force interaction between two groups of atoms.

Results and discussion

Self-assembly behavior of water molecules during and after relaxation

Interfacial moisture has a significant impact on the relaxing process and post-relaxation state of CNCs-water system. Figure 2 shows how the configurations change at various interfacial moisture to dry mass ratio levels. The relaxation process represents the mutual absorption process between CNCs, which can be divided into two steps. Firstly, the interaction between CNCs makes the surfaces of neighboring CNCs gradually fit together. Then, they are entirely fitted and tend to stabilize. The relaxation process changes while the water molecules are added to the interfacial region. At lower interfacial moisture, as an example, in the case of 0.25 wt% interfacial moisture, the water molecules will adsorb on the adjacent surfaces of CNCs. Afterward, the adsorption process is similar to the dry interfaces in that the CNC demonstrates a fitting tendency and be close to each other until stabilized. At higher moisture to dry mass ratio, such as the 0.75 wt% case, our simulations reveal a distinct distribution of water molecules at the CNC interface. While some water molecules adsorb onto the surfaces S1 and S2, others disperse within the interfacial region between the nanocrystals. This increase in water molecule density promotes a tendency for closer packing in these regions, as evidenced by our trajectory analysis. In other words, the presence of more water molecules in these areas appears to draw the CNCs slightly closer together.
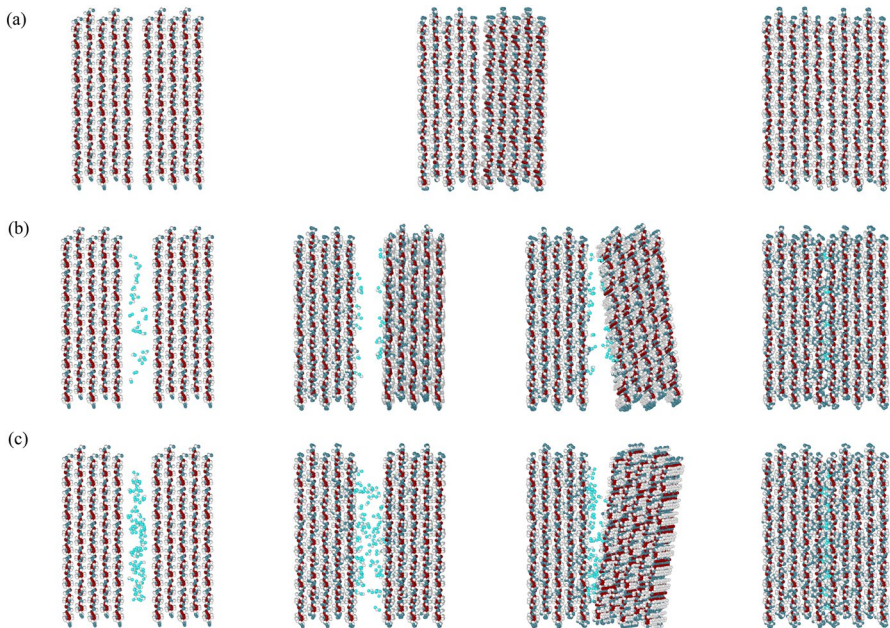

Fig. 2 **a** Dry interface relaxation process, **b** 0.25 wt% interface relaxation process, **c** 0.75 wt% interface relaxation process

After initial relaxation, the water molecules are located between the seams of CNCs. As illustrated in Fig. 3, the chains of CNCs can maintain their parallel orientation in both diagonal direction and vertical directions. In the interface area, the chains belonging to different CNCs are interleaved, creating gaps between CNCs, resembling a gear mesh. As moisture is introduced into the interfacial region, water molecules are adsorbed in these gaps after relaxation. With increasing moisture to dry mass ratio, the water molecules gradually spread throughout the interface but still concentrate in the gap region, as shown in Fig. 3b–f. It is noteworthy that while the arrangement of CNC system appears to be relatively orderly in the dry state, the arrangement of atoms in the CNC-water system becomes chaotic. As shown in Fig. 3, an increase in interfacial moisture can lead to the gradual and uniform dispersion of water molecules between the CNC interface. However, this increase in moisture to dry mass ratio may also enlarge the gap between the CNCs weakening the interaction.

Effects of moisture on the interface shear traction–separation behavior

The shear simulations were conducted to estimate the effect of moisture on the stick–slip behavior of CNCs. A series of 10 individual samples was used to generate the data, with the averaged curves plotted in Fig. 4. Figure 4a shows the traction–separation response along the shear direction. All curves show the stick–slip phenomenon of the CNC interface. The shear curves alter periodically where the
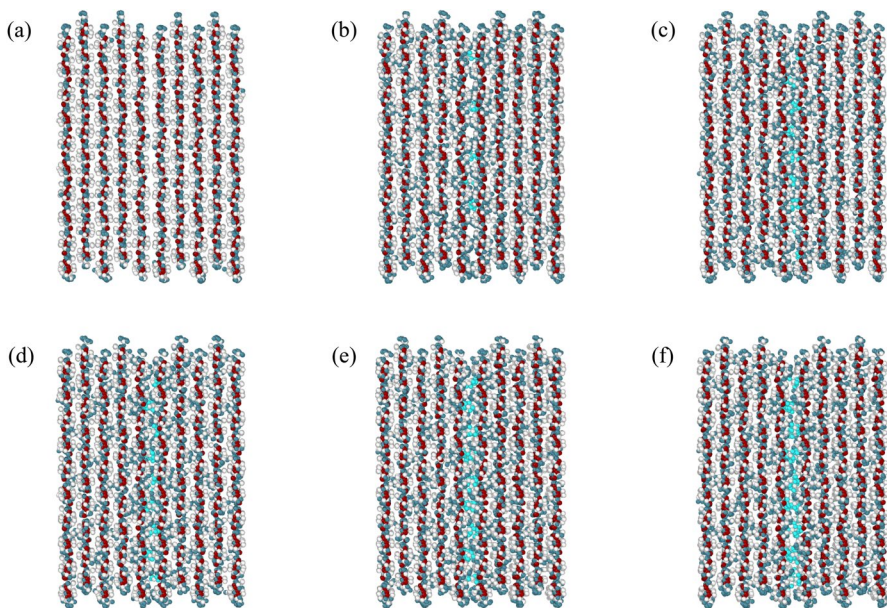

Fig. 3 Configuration of CNC-water system of different moisture: **a** Dry, **b** 0.25 wt%, **c** 0.5 wt%, **d** 0.75 wt%, **e** 1.0 wt%, **f** 1.25 wt%
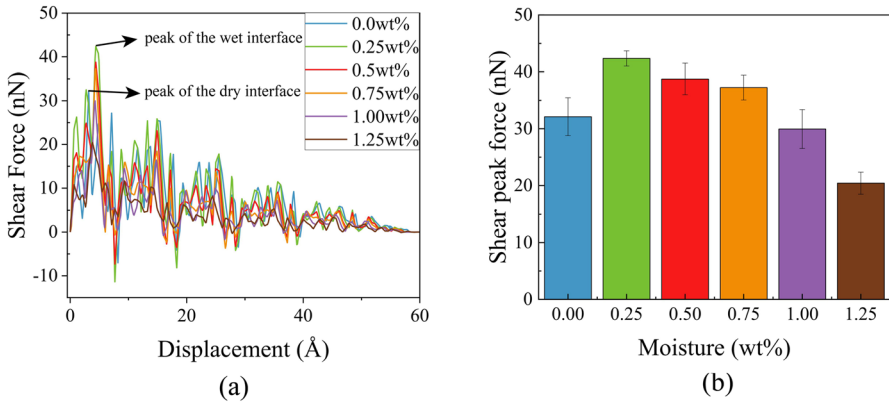
Fig. 4 Interfacial shear mechanical property of CNC interface: **a** force-displacement curves of shearing loading at different moisture situations, **b** shear peak force of different moisture situations

displacement is the multiple of the length of the cellulose units. Figure 4a shows the difference in shear force–displacement curves for both dry and wet interfaces. These curves exhibit a series of force peaks that gradually diminish in magnitude. This observation is due to a progressive decrease in the effective interaction area between the CNCs as they slide past each other during shearing. The initial peak in the dry interface curve occurs at approximately 5 Å, which corresponds to half the length of a cellobiose unit. Specifically, a rise of 5.19 Å per residue corresponds to a total length of 10.38 Å for a cellobiose unit, as reported by a previous study (Nishiyama et al. 2002). The positions of these peaks show an oscillating pattern, corresponding to the periodic crystalline structure of cellulose. The wet interface exhibits a slightly distinct behavior. The peak force is slightly delayed compared to the dry interface, and the overall force variation becomes smoother as the moisture to dry mass ratio become higher. This observation aligns with our finding that water molecules fill the gaps between CNCs during equilibration. The presence of water likely alters the interaction patterns between CNCs, causing a more gradual increase and decrease in shear force. Consequently, the wet interface requires a slightly larger displacement to reach the peak force from the equilibrating state, indicating a more complex interaction due to moisture. In conclusion, the introduction of water molecules results in a smoother and slightly delayed force profile in the wet interface shear response.

The shear peak force of different moisture situations is shown in Fig. 4b. The interface exhibits higher shear peak force in low moisture to dry mass ratio cases (from 0.25 wt% to 0.75 wt%) compared to the dry interface. However, the shear peak force decreases when the moisture to dry mass ratio exceeding 0.75 wt%. As shown in Fig. 4a–b, the shear peak force gradually reduces with the addition of moisture and the amplitude of oscillation of the curves decreases in all wet cases. This suggests the addition of water molecules reduces the interaction, thereby diminishing the stick–slip function of CNCs. During shear deformation, the behavior of the water molecules is quite different. When the moisture is

lower than 1.0 wt%, the gap between the interface shrinks and the shear barrier increases. Consequently, the water functions as the binder of the CNC interface. Therefore, larger shear force is required to overcome the enhanced anti-shear ability. According to a previous study, with the increased moisture to dry mass ratio, the vacancy between the interface is occupied and forms a water-related hydrogen bond network between the CNCs, as shown in Fig. 5, and the water hydrogen bonds are more unstable and fleeting compared with the CNCs hydrogen bonds (Wei et al. 2018). As a result, the interaction between the CNCs is weakened due to the decrease in the h-bond stability. Considering the behavior of water molecules, some of the water molecules roll along the shear path instead of contributing to the interfacial shear peak force. Although the force–displacement curves are similar in shape, the curves gradually become smoother due to the low stability of the hydrogen bonds formed by water combined with the reduced vdW interaction between CNC interfaces. In such conditions, the CNC interface exhibits weaker resistance to shear deformation while the water works as lubricant. A similar trend had been observed by Wei et al. (2018) and Sinko and Keten (2014), where the water could increase the shear peak force and then significantly decrease the shear peak force.
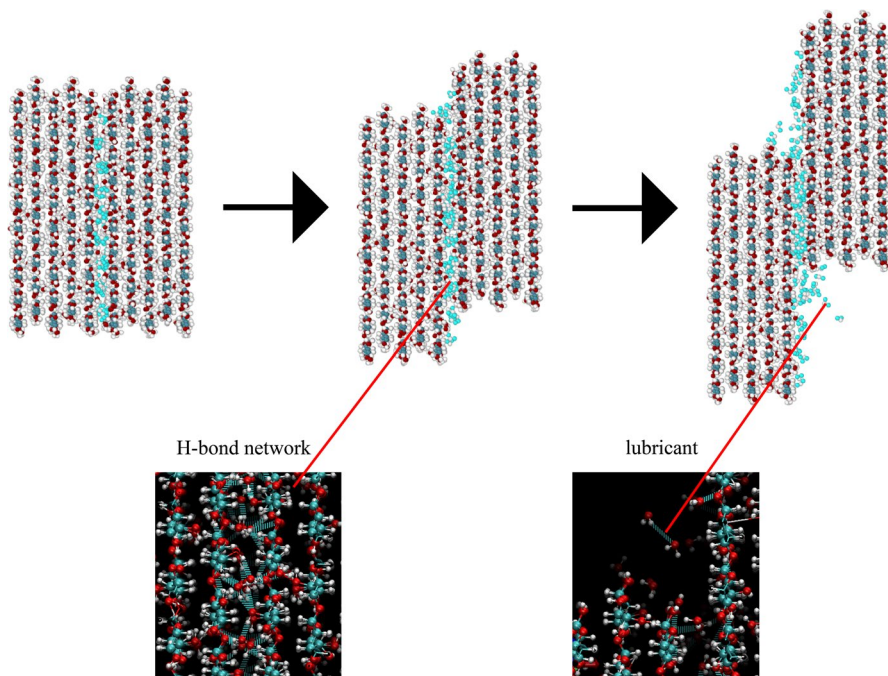

Fig. 5 Shearing process of 1.25 wt% case with the hydrogen bonds network formed by water molecules and CNC, some water molecules work as lubricant between CNC interfaces

Effects of moisture on the interface tensile traction–separation behavior

The results of the tensile simulation of CNC interfaces are presented in Fig. 6a–b to demonstrate the behavior of water molecules during separation and explain how the interfacial property changes. What stands out in Fig. 6b is the different interfacial tensile peak force of samples with different moisture to dry mass ratio. The tensile peak force shows a similar trend to the shear peak force. The peak force appears in 0.25 wt% case with interfacial peak force being 116.5 nN. After that, there has been a gradual fall in the peak force instead of a sharp drop in shear mode. Furthermore, unlike the case of shear, the interfacial peak force of 1.0% samples is still larger than the dry interfaces.

Based on previous studies (Sinko and Keten 2015; Sinko et al. 2014), it is believed that the van der Waals interaction is the dominant interaction mechanism for 200–200 interface of CNCs. As discussed in the section about self-assembly behavior of CNC system, water molecules of low moisture attract the CNCs closer to each other, this effect enhances the van der Waals interaction leading to the increase in the separation force. Previous studies have shown that cellulose exhibits a limited capacity for water adsorption, with excess moisture remaining in a free state (Paajanen et al. 2022; Petridis et al. 2014). Our simulations are consistent with these studies, indicating that at high moisture levels, the adsorption sites on the S1 and S2 surfaces become saturated, leading to the presence of unbound water molecules. Analyses of the simulation trajectories for the separation process at 0.5 wt% and 1.0 wt% cases support these observations. As shown in Fig. 7, upon complete separation of the CNCs, while the water molecules remain adsorbed to the surfaces at 0.5 wt%, a portion of the water molecules at 1.0 wt% disperse within the space between CNCs.

Moreover, in force–displacement curves, there appears a second peak in each curve as shown in Fig. 6a. Figure 8a, b show the relationship of separation force and number of hydrogen bonds of 1.0 wt% case and 1.25 wt% case. The trend how the
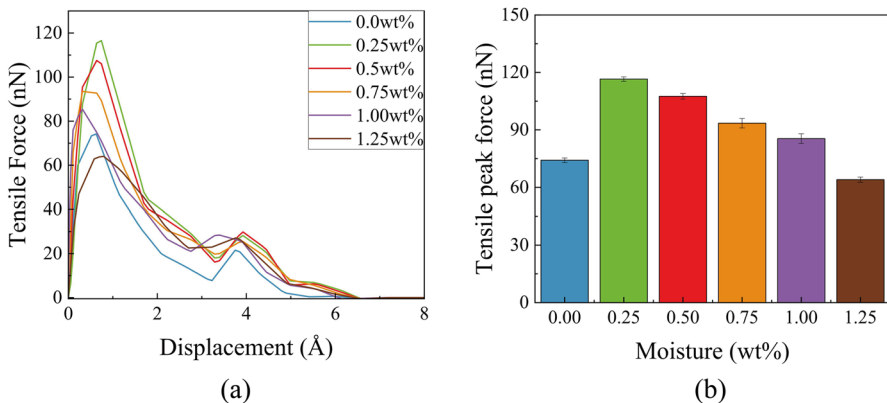

Fig. 6 Interfacial tensile mechanical property of CNC interface: **a** force-displacement curves of tensile loading at different moisture situations, **b** tensile peak force of different moisture situation
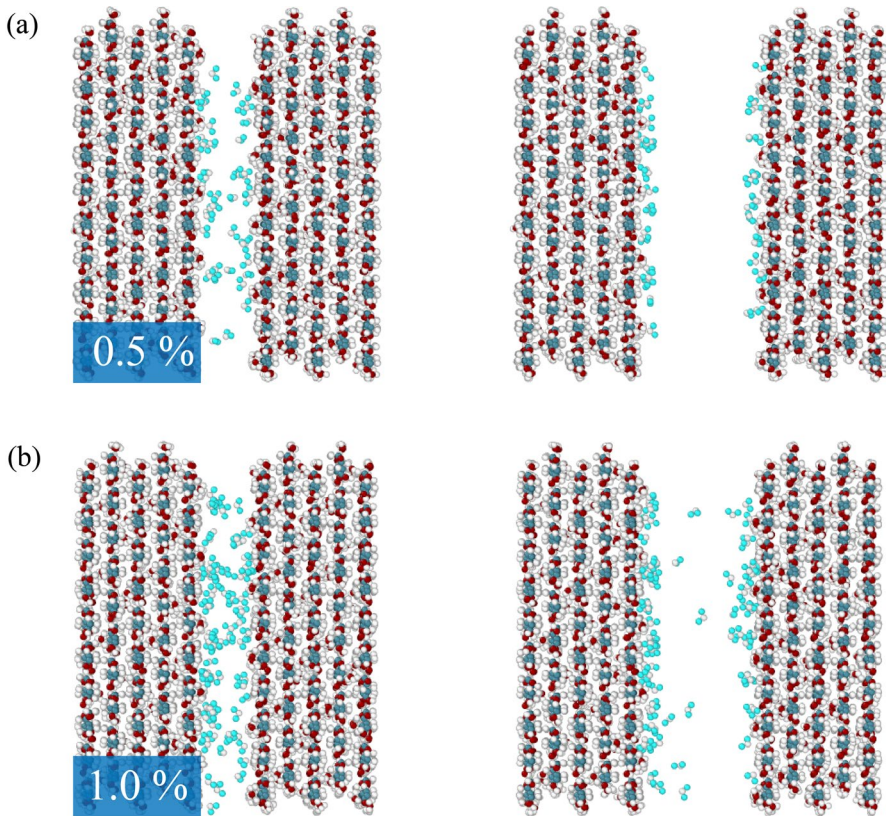
Fig. 7 Schematic representation of interface separation: **a** 0.5 wt% and **b** 1.0 wt%
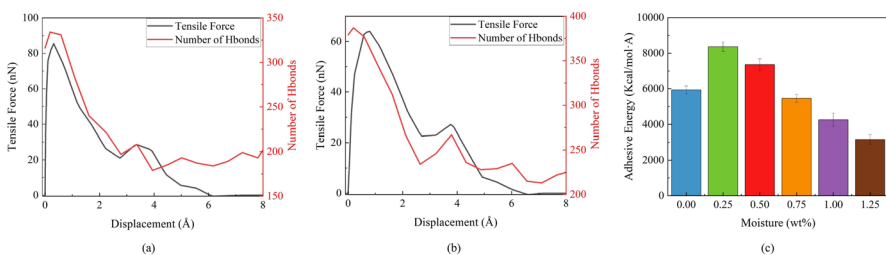

Fig. 8 **a** Relationship between tensile force and number of hydrogen bonds of 1.0 wt% case, **b** relationship between tensile force and number of hydrogen bonds of 1.25 wt%, **c** adhesive energy of different moisture situations

curves change is almost the same. As discussed before, during the 200–200 interface separation process, the van der Waals interaction plays a dominant role which is only related to distance. With the separation of interfaces, the van der Waals interaction decreases, so the second peak in the force–displacement curve is irrelevant for van

der Waals interaction. From Fig. 8a, b it can be seen that the second peak appears in the force–displacement curve following a peak in the hydrogen bond-displacement curve. Although hydrogen bonds are not the main interaction of 200–200 interface, their attracting effect on the interfaces still needs to be overcome in the separation process. Figure 7 shows a schematic diagram of the internal hydrogen bond during separation. With the increase of moisture, the hydrogen bonds network structure becomes more complicated. In the sample of 1.0 wt% moisture to dry mass ratio, there are plenty of lines between the CNC interfaces connected by multiple water molecules consisting of more than two hydrogen bonds. In 0.5 wt% case most of the hydrogen bonds formed by water are CNC-water h-bond or CNC-water-CNC h-bond.

Figure 8c demonstrates the adhesive energy of different moisture to dry mass ratio interfaces. The adhesive energy exhibits the same trend as the interfacial peak force, which increases first and then descends afterwards. As described before, the addition of water molecules can draw the two CNCs closer to each other and lead to the increase in adhesive energy. While the interfacial moisture increasing further, the adhesive energy descends by opening the gap between the CNCs, which replaces the CNC-CNC hydrogen bonds by CNC-water-CNC hydrogen bonds and reduces the vdW interactions. In this case, the 0.25 wt% moisture to dry mass ratio is a special state for the CNC system in our study, which reaches the maximum vdW interaction and hydrogen bond interaction. When the external load acts on this CNC system, greater forces are required to overcome the interaction within the system, therefore the adhesive energy, shear peak force and tensile peak force are maximum.

Effects of temperature on dry and wet interface

To systematically analyze the effects of temperature on the interfacial property of CNC interface, we employed simulations for both dry and wet conditions. Ten simulations of each condition were employed and averaged to ensure accuracy.

Effect of temperature on dry interface

Figure 9 illustrates the interfacial properties of the dry CNC interface at different temperatures. The model and simulation details used in this section are the same as those in the last section. Unlike the effect of moisture to dry mass ratio on the interfacial properties, there is no clear regularity in the variation trend of the interfacial properties with temperature. The shear peak force of the dry interface decreases as the temperature increases. After reaching 320 K, the shear peak force begins to rise and then declines at 350 K, as shown in Fig. 9a. In terms of the tensile peak force, as presented in Fig. 9b, there are no significant changes observed from 300 to 340 K. However, at 350 K, the tensile peak force slightly decreasing compared to room temperature. The adhesive energy exhibits an initial increase followed by a decrease trend, as depicted in Fig. 9c. Based on the above description, the influence of temperature on the interfacial properties is unstable, and the changing trends of shear peak force and tensile peal force differ considerably. The
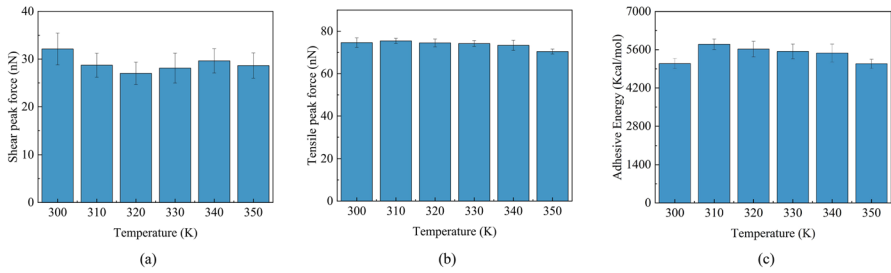
Fig. 9 **a** Shear peak force of dry CNC interface at different temperature, **b** tensile peak force of dry interface at different temperature, **c** adhesive energy of dry CNC interface at different temperature

variation in adhesive energy is similar to that of moisture, but overall, the changes in interfacial properties are not significant. Therefore, within the temperature range studied in this paper, there is no apparent influence of temperature on the interfacial mechanical properties of dry interface.

Effect of temperature on wet interface

In this part, we estimate the effects of temperature on the wet interface. To comprehensively investigate the combined effects of temperature and moisture on the CNC interface, this study examined the temperature range of 300–350 K, consistent with previous section. Given the distinct water molecule behavior across varying moisture levels, multiple moisture conditions, ranging from 0.25 wt% to 1.5 wt%, were incorporated into the study.

The variation of the interfacial shear peak force is shown in Fig. 10, where the fluctuation of the mechanical properties varies for different moisture conditions. At
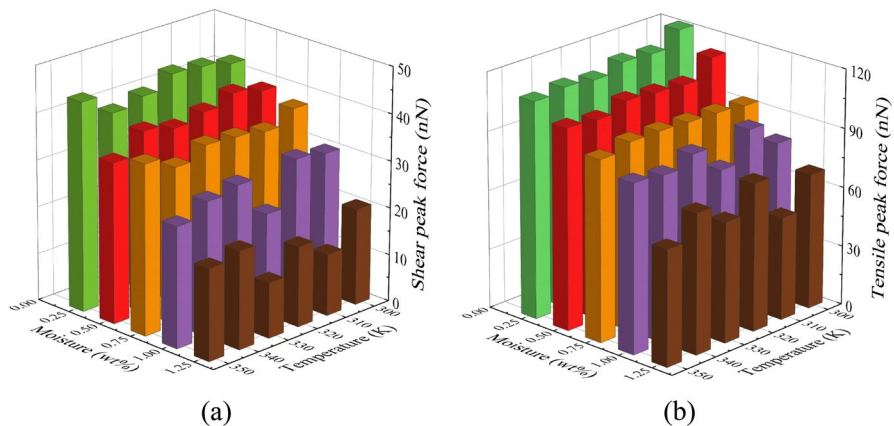

Fig. 10 **a** Shear peak force of all moisture situations at different temperatures, **b** tensile peak force of all moisture situations at different temperatures

lower moisture level (from 0.25 wt% to 0.75 wt%), little fluctuation in the variation of the shear peak force is observed, but at higher levels (1.0 wt% and 1.25 wt%), the change of the shear peak force with temperature becomes considerable and there are some abnormal situations, such as 320 K at 1.0 wt% moisture and 310 K at 1.25 wt%. At low interfacial moisture, the difference between the maximum and minimum shear peak force is 11% and 18.26% respectively. At high moisutre, the difference between the maximum shear peak force and minimum ones is 44.23% and 76.46% respectively. This result illustrates the instability of the interfacial mechanical properties of CNC interface at high temperature and moisture situations. In general, the shear peak force shows a trend of increasing and then decreasing. The phenomenon also appears in the variation of the tensile peak force. At low moisture, the tensile peak force of the CNC interface decreases gradually with the increasing of temperature. The smallest change in tensile peak force occurs at 0.75 wt% moisture. At high moisture, the fluctuation in tensile peak force becomes greater. At low moisture the maximum values of tensile peak force increase by 10.14% and 11% respectively compared to the minimum values. At moisture of 1.25 wt%, the maximum value of tensile peak force increases by 44.34% compared to the minimum value.

The adhesive energy of the CNC interface is given in Fig. 11. The general trend of the relevant changes in adhesive energy is similar to that of the interfacial peak force. The adhesive energy is larger at lower temperatures and moisture. The change in the adhesive energy is smallest at 0.75% moisture, showing a trend of increasing and then decreasing. The effect of temperature on the adhesive becomes more significant at higher interfacial moisture, especially at 1.25 wt%. When the interfacial moisture reached 1.25 wt%, the adhesive energy represents a significant change from 320 to 330 K, decreasing by 27.5%. As the temperature further increases, the interfacial adhesive energy decreases to a lower level.

This section outlines the results of the temperature impact on different moisture of CNC interface performance. At low moisture level, the interfacial property changes slightly. When the moisture increases, the impact of temperature on interfacial

Fig. 11 Adhesive energy of all moisture situations at different temperature
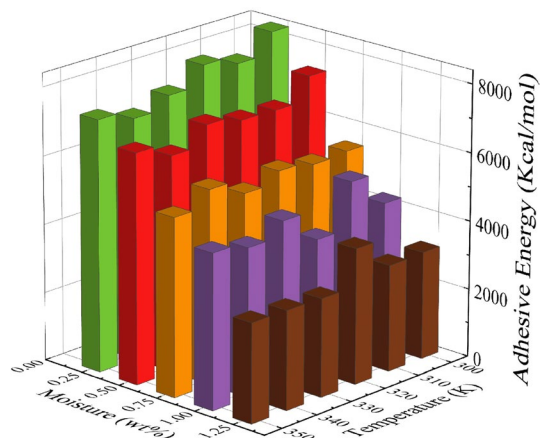
performance become more considerable. The key finding in this section is that the effect of temperature on the interfacial shear property is more pronounced compared to its effect on tensile property at high moisture levels. We observed a trend of increasing and then decreasing under certain conditions. In general, the combined effect of temperature and moisture on the mechanical properties at CNC interface is complex. Temperature has a similar impact on the interface at low moisture levels as it does on dry condition, but its effect becomes more pronounced at high moisture levels.

Conclusion

In this work, molecular dynamics (MD) simulations were conducted to investigate the effects of moisture and temperature on the CNC interface. The simulations focused on understanding the interfacial mechanical properties and behavior of CNC interface under both tensile and shear loading across different temperature and moisture conditions. The major conclusions are drawn as follows:

(1) The configuration of CNC interface changes considerably while the moisture increases from 0.0 wt% to 1.25 wt%. At low moisture, the water molecules may occupy the vacancy between CNCs and lead the CNCs closer to each other. This also may enhance the interaction of CNCs. When the moisture at the interface increases, the vacancy is completely occupied by water molecules and the distance between CNC is propped up. As a result, the interaction constantly declines.

(2) At room temperature, the interfacial mechanical properties show an increasing and then descending trend with the increasing interfacial moisture. At low moisture levels, the water molecules work as a binder that expands the van der Walls interaction between the CNC which is the domain interaction of 200–200 interface. At high moisture levels, the water molecules become lubricant because they substantially lower the adhesive energy and peak force between CNC interface.

(3) The effects of temperature are slight for dry and low moisture cases. As for the comparatively high moisture cases, the effects of temperature are more significant on shear rather than tensile properties. In general, the effects of temperature on the interfacial mechanical properties are not uniform at the temperature range studied in this paper. Further and comprehensive researches ought to be conducted to deeply probe the combine effect of temperature and moisture on the CNC interfacial performance.

This study provides insights into the shear and tensile performance of CNCs interfaces at different interfacial moisture and temperature. Our investigation implies that CNCs with a better interfacial performance can be obtained by controlling the moisture and temperature, which may be used to provide fundamental recommendation for the design and application of CNCs.

Declarations

References

Adak B, Mukhopadhyay S (2018) All-cellulose composite laminates with low moisture and water sensitivity. Polymer 141:79–85. https://doi.org/10.1016/j.polymer.2018.02.065

Ahmad S et al (2022) Polyvinyl alcohol and aminated cellulose nanocrystal membranes with improved interfacial compatibility for environmental applications. Environ Res 214:113793. https://doi.org/10.1016/j.envres.2022.113793

Azeredo HMC, Rosa MF, Mattoso LHC (2017) Nanocellulose in bio-based food packaging applications Ind Crop. Prod 97:664–671. https://doi.org/10.1016/j.indcrop.2016.03.013

Bangar SP, Whiteside WS (2021) Nano-cellulose reinforced starch bio composite films- a review on green composites. Int J Biol Macromol 185:849–860. https://doi.org/10.1016/j.ijbiomac.2021.07.017

Bangar SP, Harussani MM, Ilyas RA, Ashogbon AO, Singh A, Trif M, Jafari SM (2022) Surface modifications of cellulose nanocrystals: processes, properties, and applications. Food Hydrocoll 130:107689. https://doi.org/10.1016/j.foodhyd.2022.107689

Bregado JL, Tavares FW, Secchi AR, Segtovich ISV (2021) Molecular dynamics of dissolution of a 36-chain cellulose Iβ microfibril at different temperatures above the critical pressure of water. J Mol Liq 336:116271. https://doi.org/10.1016/j.molliq.2021.116271

Choi JY et al (2021) Atomistic mechanisms of adhesion and shear strength in graphene oxide-polymer interfaces. J Mech Phys Solids 156:104578. https://doi.org/10.1016/j.jmps.2021.104578

Dri FL, Wu X, Moon RJ, Martini A, Zavattieri PD (2015) Evaluation of reactive force fields for prediction of the thermo-mechanical properties of cellulose Iβ. Comp Mater Sci 109:330–340. https://doi.org/10.1016/j.commatsci.2015.06.040

Du D, Tang C, Tang Y, Yang L, Hao J (2021) Molecular simulation on the mechanical and thermal properties of carbon nanowire modified cellulose insulating paper. Compos Struct 261:113283. https://doi.org/10.1016/j.compstruct.2020.113283

Eichers M, Bajwa D, Shojaeiarani J, Bajwa S (2022) Biobased plasticizer and cellulose nanocrystals improve mechanical properties of polylactic acid composites. Ind Crop Prod 183:114981. https://doi.org/10.1016/j.indcrop.2022.114981

Garg M, Linares M, Zozoulenko I (2020) Theoretical rationalization of self-assembly of cellulose nanocrystals: effect of surface modifications and counterions. Biomacromol 21:3069–3080. https://doi.org/10.1021/acs.biomac.0c00469

Gomes TCF, Skaf MS (2012) Cellulose-builder: a toolkit for building crystalline structures of cellulose. J Comput Chem 33:1338–1346. https://doi.org/10.1002/jcc.22959

He Z, Wu H, Xia J, Hou Y, Zhu Y (2023) How weak hydration interfaces simultaneously strengthen and toughen nanocellulose materials extreme. Mech Lett 58:101947. https://doi.org/10.1016/j.eml.2022.101947

Huang F, Wei W, Fan Q, Li L, Zhao M, Zhou Z (2022) Super-stretchable and adhesive cellulose nanofiber-reinforced conductive nanocomposite hydrogel for wearable motion-monitoring sensor. J Colloid Interf Sci 615:215–226. https://doi.org/10.1016/j.jcis.2022.01.117

Humphrey W, Dalke A, Schulten K (1996) VMD: visual molecular dynamics. J Mol Graph 14(33–38):27–28. https://doi.org/10.1016/0263-7855(96)00018-5

Jakob M, Mahendran AR, Gindl-Altmutter W, Bliem P, Konnerth J, Müller U, Veigel S (2022) The strength and stiffness of oriented wood and cellulose-fibre materials: a review. Prog Mater Sci 125:100916. https://doi.org/10.1016/j.pmatsci.2021.100916

Jiang Y, Lawrence M, Hussain A, Ansell M, Walker P (2019) Comparative moisture and heat sorption properties of fibre and shiv derived from hemp and flax. Cellulose (London) 26:823–843. https://doi.org/10.1007/s10570-018-2145-0

Kang HJ, Yang N, Song YS (2024) Enhanced thermal, mechanical, and optical properties of cellulose nanocrystal embedded cyclic olefin copolymer composite film. Korea-Aust Rheol J. https://doi.org/10.1007/s13367-024-00095-0

Khoshkava V, Kamal MR (2014) Effect of drying conditions on cellulose nanocrystal (CNC) agglomerate porosity and dispersibility in polymer nanocomposites. Powder Technol 261:288–298. https://doi.org/10.1016/j.powtec.2014.04.016

Li Y et al (2019) Modeling the effects of interfacial properties on the temperature dependent tensile strength of fiber reinforced polymer composites. Compos Sci Technol 172:74–80. https://doi.org/10.1016/j.compscitech.2019.01.011

Li W, Chai W, Zhang L, Guo Y, Wang W, Chen S (2022) Atomic insight into the influences of moisture ingress on the structures and dynamics of graphene-epoxy interfaces. Compos Sci Technol 219:109222. https://doi.org/10.1016/j.compscitech.2021.109222

Long Z et al (2022) Influence of sea salt on the interfacial adhesion of bitumen–aggregate systems by molecular dynamics simulation. Constr Build Mater 336:127471. https://doi.org/10.1016/j.conbuildmat.2022.127471

Martinez L, Andrade R, Birgin EG, Martinez JM (2009) Software news and update packmol: a package for building initial configurations for molecular dynamics simulations. J Comput Chem 30(13):2157–2164

Meng Q, Shi X (2021) A microstructure-based constitutive model of anisotropic cellulose nanopaper with aligned nanofibers. Extreme Mech Lett 43:101158. https://doi.org/10.1016/j.eml.2020.101158

Mianehrow H, Berglund LA, Wohlert J (2022) Interface effects from moisture in nanocomposites of 2D graphene oxide in cellulose nanofiber (CNF) matrix – a molecular dynamics study. J Mater Chem A 10:2122–2132. https://doi.org/10.1039/D1TA09286C

Molnár G, Rodney D, Martoïa F, Dumont PJJ, Nishiyama Y, Mazeau K, Orgéas L (2018) Cellulose crystals plastify by localized shear. Proc Natl Acad Sci 115:7260–7265. https://doi.org/10.1073/pnas.1800098115

Moon RJ, Martini A, Nairn J, Simonsen J, Youngblood J (2011) Cellulose nanomaterials review: structure, properties and nanocomposites. Chem Soc Rev 40:3941–3994. https://doi.org/10.1039/c0cs00108b

Naito K, Nagai C (2022) Effects of temperature and water absorption on the interfacial mechanical properties of carbon/glass-reinforced thermoplastic epoxy hybrid composite rods. Compos Struct 282:115103. https://doi.org/10.1016/j.compstruct.2021.115103

Nishiyama Y, Langan P, Chanzy H (2002) Crystal structure and hydrogen-bonding system in cellulose Iβ from synchrotron x-ray and neutron fiber diffraction. J Am Chem Soc 124:9074–9082. https://doi.org/10.1021/ja0257319

Oehme DP, Downton MT, Doblin MS, Wagner J, Gidley MJ, Bacic A (2015) Unique aspects of the structure and dynamics of elementary Iβ cellulose microfibrils revealed by computational simulations. Plant Physiol 168:3–17. https://doi.org/10.1104/pp.114.254664

Paajanen A, Zitting A, Rautkari L, Ketoja JA, Penttilä PA (2022) Nanoscale mechanism of moisture-induced swelling in wood microfibril bundles. Nano Lett 22:5143–5150. https://doi.org/10.1021/acs.nanolett.2c00822

Pan J, Wei N, Zhao J (2019) Shear properties of the liquid bridge between two graphene films using a refined molecular kinetics theory and molecular dynamics simulations. Mech Mater 137:103124. https://doi.org/10.1016/j.mechmat.2019.103124

Patel DK, Dutta SD, Hexiu J, Ganguly K, Lim K (2020) Bioactive electrospun nanocomposite scaffolds of poly(lactic acid)/cellulose nanocrystals for bone tissue engineering. Int J Biol Macromol 162:1429–1441. https://doi.org/10.1016/j.ijbiomac.2020.07.246

Petridis L et al (2014) Hydration control of the mechanical and dynamical properties of cellulose. Biomacromol 15:4152–4159. https://doi.org/10.1021/bm5011849

Ren Y, Ma J, Liu W, Huang C, Lai C, Ling Z, Yong Q (2022) Facile adjustment on cellulose nanocrystals composite films with glycerol and benzyl acrylate copolymer for enhanced UV shielding property. Int J Biol Macromol 204:41–49. https://doi.org/10.1016/j.ijbiomac.2022.01.168

Sahputra IH, Alexiadis A, Adams MJ (2019) Effects of moisture on the mechanical properties of microcrystalline cellulose and the mobility of the water molecules as studied by the hybrid molecular mechanics-molecular dynamics simulation method. J Polym Sci B Polym Phys 57:454–464. https://doi.org/10.1002/polb.24801

Shen P, Tang Q, Chen X, Li Z (2022) Nanocrystalline cellulose extracted from bast fibers: preparation, characterization, and application. Carbohyd Polym 290:119462. https://doi.org/10.1016/j.carbpol.2022.119462

Shishehbor M, Dri FL, Moon RJ, Zavattieri PD (2018) A continuum-based structural modeling approach for cellulose nanocrystals (CNCs). J Mech Phys Solids 111:308–332. https://doi.org/10.1016/j.jmps.2017.11.006

Sinko R, Keten S (2014) Effect of moisture on the traction-separation behavior of cellulose nanocrystal interfaces. Appl Phys Lett 105:243702. https://doi.org/10.1063/1.4904708

Sinko R, Keten S (2015) Traction–separation laws and stick–slip shear phenomenon of interfaces between cellulose nanocrystals. J Mech Phys Solids 78:526–539. https://doi.org/10.1016/j.jmps.2015.02.012

Sinko R, Mishra S, Ruiz L, Brandis N, Keten S (2014) Dimensions of biological cellulose nanocrystals maximize fracture strength. ACS Macro Lett 3:64–69. https://doi.org/10.1021/mz400471y

Stukowski A (2010) Visualization and analysis of atomistic simulation data with OVITO–the open visualization tool. Model Simul Mater Sci Eng 18:15012. https://doi.org/10.1088/0965-0393/18/1/015012

Tang J, Sisler J, Grishkewich N, Tam KC (2017) Functionalization of cellulose nanocrystals for advanced applications. J Colloid Interf Sci 494:397–409. https://doi.org/10.1016/j.jcis.2017.01.077

Thompson AP et al (2022) LAMMPS - a flexible simulation tool for particle-based materials modeling at the atomic, meso, and continuum scales. Comput Phys Commun 271:108171. https://doi.org/10.1016/j.cpc.2021.108171

Wang Q, Sun J, Yao Q, Ji C, Liu J, Zhu Q (2018) 3D printing with cellulose materials. Cellulose 25:4275–4301. https://doi.org/10.1007/s10570-018-1888-y

Wei Z, Sinko R, Keten S, Luijten E (2018) Effect of surface modification on water adsorption and interfacial mechanics of cellulose nanocrystals. Acs Appl Mater Inter 10:8349–8358. https://doi.org/10.1021/acsami.7b18803

Xu Y, He L, Xie Z, Wang Z, Chen Y, Wu Q (2024) Influence of PEG on toughness, humidity sensitivity and structural color of cellulose nanocrystal films. Cellulose (London). https://doi.org/10.1007/s10570-024-06035-z

Yang J, Li J (2018) Self-assembled cellulose materials for biomedicine: a review. Carbohyd Polym 181:264–274. https://doi.org/10.1016/j.carbpol.2017.10.067

Zhang C, Chen M, Keten S, Coasne B, Derome D, Carmeliet J (2021a) Hygromechanical mechanisms of wood cell wall revealed by molecular modeling and mixture rule analysis. Sci Adv 7:i8919. https://doi.org/10.1126/sciadv.abi8919

Zhang C, Keten S, Derome D, Carmeliet J (2021b) Hydrogen bonds dominated frictional stick-slip of cellulose nanocrystals. Carbohyd Polym 258:117682. https://doi.org/10.1016/j.carbpol.2021.117682

Zhao H, Dai X, Yuan Z, Li G, Fu Y, Qin M (2022) Iridescent chiral nematic papers based on cellulose nanocrystals with multiple optical responses for patterned coatings. Carbohyd Polym 289:119461. https://doi.org/10.1016/j.carbpol.2022.119461

Zhou Y, Stuart-Williams H, Farquhar GD, Hocart CH (2010) The use of natural abundance stable isotopic ratios to indicate the presence of oxygen-containing chemical linkages between cellulose and lignin in plant cell walls. Phytochemistry 71:982–993. https://doi.org/10.1016/j.phytochem.2010.03.001

Zhou A, Tam L, Yu Z, Lau D (2015) Effect of moisture on the mechanical properties of CFRP–wood composite: an experimental and atomistic investigation. Compos b: Eng 71:63–73. https://doi.org/10.1016/j.compositesb.2014.10.051

Zhu H et al (2015) Anomalous scaling law of strength and toughness of cellulose nanopaper. Proc Natl Acad Sci 112:8971–8976. https://doi.org/10.1073/pnas.1502870112